15th Australasian Fluid Mechanics Conference
The University of Sydney, Sydney, Australia
13-17 December 2004

Velocity Distribution in an Asymmetric Diffuser With Perforated Plates

M.N. Noui-Mehidi, J. Wu and I. Sutalo
Fluids Engineering Division, CSIRO, Manufacturing and Infrastructure Technology
PO Box 56, Graham Rd, Highett, Vic, 3190 AUSTRALIA

Abstract

An experimental investigation has been carried out to study the use of perforated plates to control the velocity distribution at the outlet of a wide-angle asymmetric diffuser. The diffuser was half a pyramidal diffuser, the inner wall of which was parallel to the flow, while the other was inclined. The diffuser opening angles were horizontally 45° and vertically 30° and the area ratio was equal to 7. A combination of four perforated plates with porosities of 45% resulted in differing velocity distributions at the outlet of the diffuser. Laser Doppler velocimetry measurements and wall static pressure results indicated the existence of different flow regimes when the perforated plates were placed at different locations. Velocity distributions investigated within the diffuser showed a complicated flow pattern between the different combinations of perforated plates.

Introduction

Flow control involving perforated plates and wire gauze screens in internal flows has been extensively investigated for more than 50 years [1]. Particular interest has been given to wide-angle diffusers because of their association in many applications, for example in electrostatic precipitators (ESPs) and wind tunnels. There is a natural tendency of a wide-angle diffuser to develop a highly non-uniform velocity distribution at the outlet. Therefore, there is a need to control the flow for industrial applications, such as ESPs. Many studies were concerned with the use of wire gauze and perforated plates as flow control devices [2–3]. They showed that flow is very sensitive to the nature of the screens involved and their positions within the diffuser. Space limitation in practical situations is an important issue, and diffusers used in ESP installations have area ratios greater than 6. Sahin and Ward–Smith [4] and Sahin *et al.* [5] studied flow control by perforated plates in wide-angle diffusers of ESPs with larger area ratios up to 10. In a systematic investigation of the flow distributions at the outlet of wide-angle diffusers with area ratio of 10, Ward–Smith *et al.* [6] showed that good flow uniformity can be achieved at the outlet by using only two perforated plates or wire gauze screens with appropriate porosities and locations. They proposed that two perforated plates with porosities of between 40% and 50% be used, with the first one placed at a location near one-third of the diffuser length from the inlet, and the other one at a location just prior to the diffuser exit. In the present study, the flow within a wide-angle diffuser, which can be schematically represented as half a classical pyramidal diffuser, is investigated. The inner wall is aligned with the flow and the outer wall has an opening angle of 45°. Miller [7] referred to this type of diffuser as asymmetric, but presented only a few data points since they have not been previously investigated. The purpose of this study is to investigate the effect of perforated plates on the flow distributions within this asymmetric wide-angle diffuser model. A combination of different perforated plates permitted the investigation of flow control, and the velocity distribution at the outlet of the diffuser.

Test Rig

A water circulation loop was set up to join a half-pyramidal diffuser with the inner wall parallel to the flow and the outer wall inclined with a horizontal opening angle of $\alpha = 45°$. The total divergence angle of the top and bottom walls was vertically $\beta = 30°$. The resulting outlet to inlet area ratio was therefore equal to 7. The diffuser was connected to a stainless steel box with a rectangular section of 225 × 250 mm, as shown schematically in Fig. 1. The diffuser had a length L_1 of 137 mm and the box had a length L_2 of 250 mm.

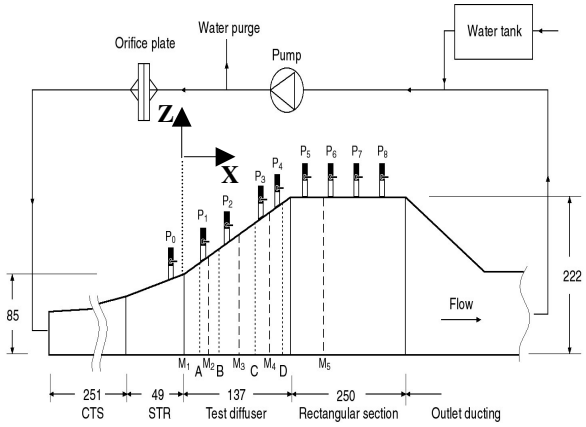

Fig.1 Experimental test rig.

Two transition ducts assured the connection of the diffuser to the upstream ducting circular pipe. The first one permitted the transition from a circular section to a semi-circular one (denoted CTS in Fig. 1), and the second duct connecting a semi-circular section to a rectangular one (denoted STR in Fig. 1). The STR duct inner wall and the diffuser inner wall, both parallel to the flow, were made from the same acrylic plate for visual access and laser Doppler velocimetry (LDV) measurements. The coordinates were defined in the Cartesian system X, Y and Z, where any (Y–Z) plane represented a section perpendicular to the flow, Y being the vertical axis; X was the downstream flow direction axis. Four slots machined into the inner sides of the diffuser stainless steel outer wall and acrylic plate (inner wall) allowed four perforated plates to be rigidly clamped vertically within the diffuser at locations $X/L_1 = 0.05$, 0.25, 0.59 and 0.95; the origin was defined at the diffuser inlet plane (M_1). The locations of the plates denoted A, B, C and D respectively, are presented in Fig. 1. The perforated plates all had the same porosity (total open area to total plate area) of 45%.

Tap water was used in the test rig. A small draining flow was placed downstream of the pump in order to avoid building up heat in the water body. A stream filled by an overhead tank permitted water loss to be compensated for.

The typical operating velocity at the diffuser inlet (M_1, Fig. 1) was 1.2 m/s, corresponding to a Reynolds number of $Re = 1.25 \times 10^5$, based on the inlet hydraulic diameter. The flow rate was measured by an orifice-plate installed downstream of the pump.

Static pressure taps were installed along the central horizontal plane of the diffuser, in order to quantify pressure variations along the flow direction. A Honeywell STD 130-EIN pressure transducer was used for pressure measurements. The locations of the pressure taps were fixed at X/L_1= –0.74, 0.02, 0.23, 0.56, 0.91, 1.18, 1.55, 2.01 and 2.39, and were denoted by P_0, P_1, P_2, P_3, P_4, P_5, P_6, P_7 and P_8 respectively. The pressure distribution is represented here by the wall static pressure loss coefficient, C_p, defined by (cf. Ward–Smith [9]):

$$C_p = \frac{P - P_r}{\frac{1}{2}\rho U_1^2} \quad (1)$$

where P is the static pressure measured at a certain location, P_r is the reference pressure located upstream to the diffuser, ρ is the water density, and U_1 is the average velocity determined at the diffuser inlet plane.

Velocity measurements were carried out using an Aerometrics one-component optical fibre LDV system. The LDV probe, which had built-in transmitting and receiving optics, was mounted on an industrial robotic arm, permitting the laser beam to be automatically positioned at the desired position within the diffuser/box combination. A 610 mm focal length lens was used for both transmitting the laser beams and collecting the scattered light from reflective magnapearl seed particles of 5–10 μm diameter. The Aerometrics system's real-time analyser allowed the reading of the mean, standard deviation and acquisition rate of the axial velocity component U along the axis X. The obtained time-mean velocity data was found to be repeatable within ±1%.

Results and Discussion

In the literature, the velocity distributions have only been measured at the outlet of diffusers. Sahin and Ward–Smith [9] discussed qualitatively the flow pattern within a wide-angle diffuser based on pressure measurements. In the present investigation, the use of a transparent inner wall for both the diffuser and box allowed axial velocity U (X) distribution measurements to be made within the diffuser and the box at different locations, indicated in Fig. 1 by M_1, M_2, M_3, M_4 and M_5. The velocity measurements were carried out using different mesh grids at each location M_i in the (Y–Z) plane. The measuring points were placed in a uniform rectangular mesh grid at each measurement section.

Empty Diffuser Flow Characteristics

In the absence of flow control, an axial jet develops within a wide-angle diffuser in the core region, and separation takes place just at the inlet due to the development of an adverse pressure gradient caused by the sudden expansion (cf. Ward–Smith [8]). In Fig. 2, mean axial velocity contours measured by LDV in a horizontal section (Y = 130 mm) through the empty diffuser in the (X–Z) plane are plotted. The figure clearly shows that the flow separates at a location of approximately X/L_1 = 0.08 from the inlet of the diffuser when there is no screen. A large recirculating zone develops in the region near the outer wall and occupies almost half the area of the measurement plane where velocity magnitudes are negative. The wall static pressure coefficient, which was negative in value as seen in Fig.3, decreased slightly along the downstream direction within the diffuser and remained unchanged in the rectangular section.

In a study of a wide-angle classical pyramidal diffuser with an expansion angle of 60°, Ward-Smith *et al.* [6] showed that the wall static pressure increased just beyond the diffuser inlet from negative to positive. This pressure recovery was not observed in our measurements.

This is probably due to the fact that our diffuser was asymmetric and had an area ratio equivalent to 14 in a pyramidal diffuser, whilst the area ratio was 10 in the work of Sahin *et al.* [5] and Ward–Smith *et al.* [6].

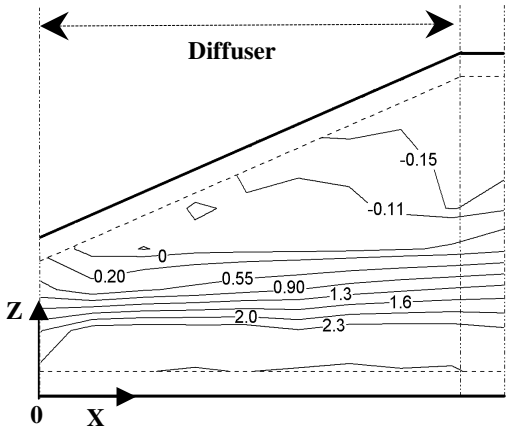

Fig.2 Velocity distribution in the asymmetric diffuser without screens in a X-Z plane (Y=130mm).

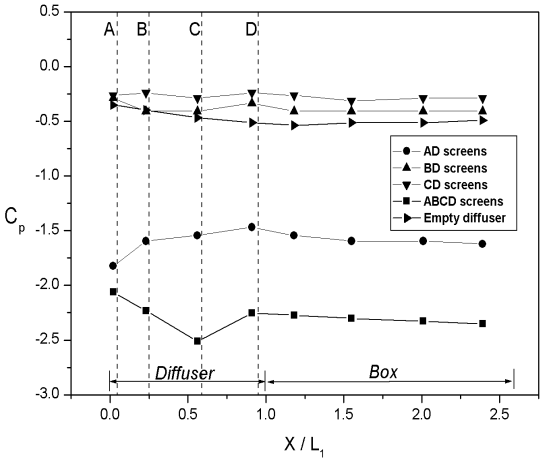

Fig.3 Downstream evolution of the pressure loss coefficient in the studied configurations.

Flow Distributions Within the Diffuser With Screens Installed

In symmetrical pyramidal diffusers Sahin and Ward–Smith [9] observed that optimal flow control could be achieved by installing a perforated plate close to the diffuser exit, with a second plate installed in an upstream location between $0.15 < X/L_1 < 0.29$ according to the present system dimensions. In the present work, four screen combinations were investigated: the first configuration had four screens installed, denoted configuration ABCD (Fig. 1). It has been studied as a limit case for comparison to the other two perforated plate configurations. In the three other configurations, screen D was fixed close to the exit of the diffuser, while another screen was installed upstream. These configurations were denoted AD, BD and CD (cf. Fig. 1). The contour plots of the mean axial velocity component U distribution within the diffuser are displayed in Figs 4–7. In each figure, four velocity distributions are presented for each of the four screen combinations studied. Each contour plot corresponds

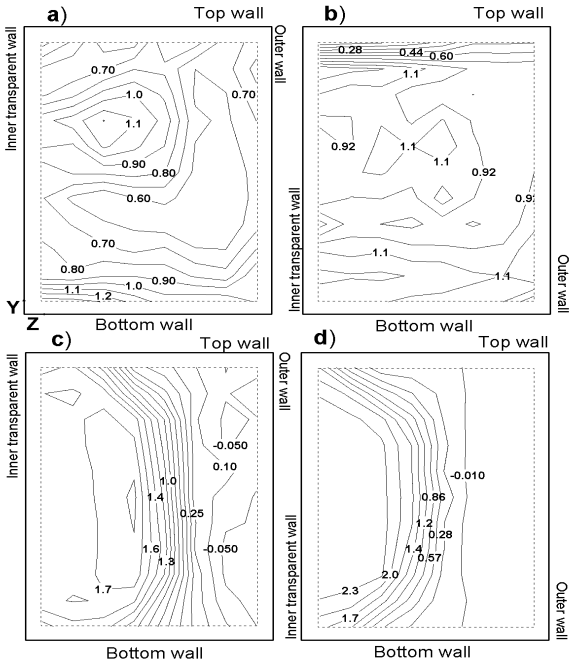

Fig.4 Velocity distributions at the section M_2.
(a) ABCD, (b) AD, (c) BD and (d) CD

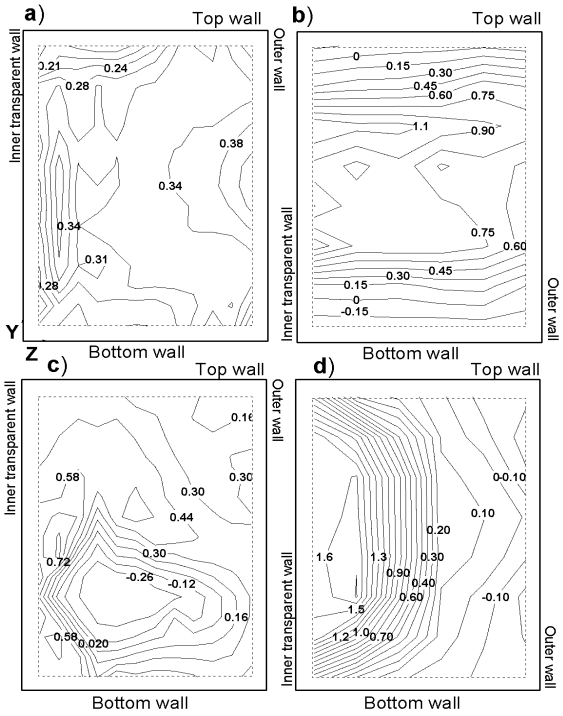

Fig.5 Velocity distributions at the section M_3.
(a) ABCD, (b) AD, (c) BD and (d) CD

to a section in the (Y–Z) plane; the velocity magnitude is given in m/s, the flow is outwards to the reader.

Figs 4a–4d represent velocity distributions taken at location M_2 for the four plate configurations. In Figs 4a and 4b the separation observed in Fig. 2 as starting at approximately X/L_1 = 0.08 was not seen due to the presence of screen A. In configuration ABCD (Fig 4a), a jet existed at the upper left corner of the section; this jet occupied the centre region in configuration AD (Fig.4b). In Figs 4c and 4d where there is no screen A, the flow separation can be clearly seen. In both configurations BD and CD, a recirculating zone developed near the outer wall, while a jet was observed near the inner wall. However, the recirculating zone in configuration CD was larger than in BD, since screen C was downstream of screen B.

In the next measuring section M_3 (Fig.5) the velocities were slowed by the second blockage corresponding to screen B in the ABCD configuration. Higher velocities are observed near the inner and outer walls (Fig.5a). In configuration AD, high velocities are confined to the core region in the measuring section, as can be seen in Fig. 5b.

In configuration BD (Fig.5c), the effect of the existence of a recirculating zone upstream of screen B can still be seen.

The recirculating zone, however, is deflected from the outer wall to occupy the lower central region of the measuring section.

The velocity distribution in configuration CD observed in Fig. 5d is similar to the one observed previously in Fig. 4d, with large recirculating zones near the outer wall. There is a decrease in the velocity magnitude as the measuring section gets closer to screen C. These results suggest that the presence of screen A prevented separation occurring and the flow remained attached downstream. In the other configurations when separation occurred, even the presence of screen B did not eliminate the recirculating zone downstream as it was deflected from the outer wall to the centre region.

Velocity distribution obtained at M_4 between the locations of screens C and D showed that the flow in configuration ABCD (Fig. 6a) was pushed towards the outer wall where high velocities existed. In configuration AD, the core region presented higher

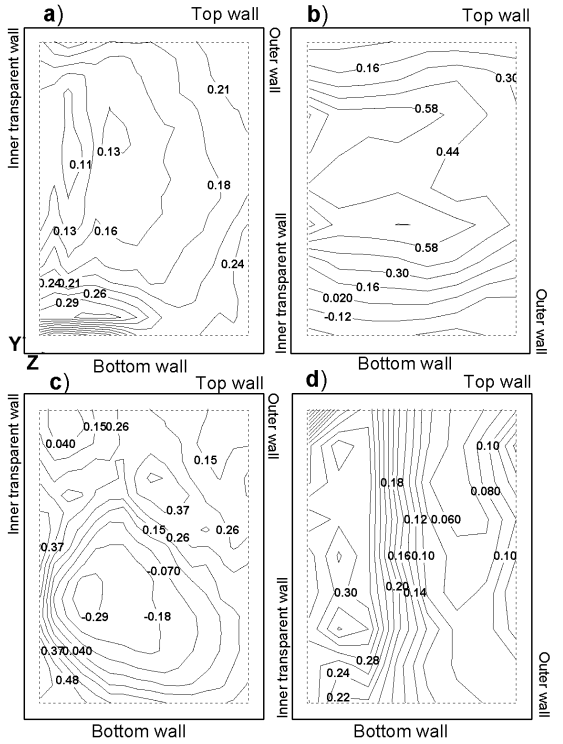

Fig.6 Velocity distributions at the section M_4
(a) ABCD, (b) AD, (c) BD and (d) CD

velocities in the measuring section (Fig. 6b). The recirculating zone observed previously in Fig. 5c is still present in Fig. 6c for

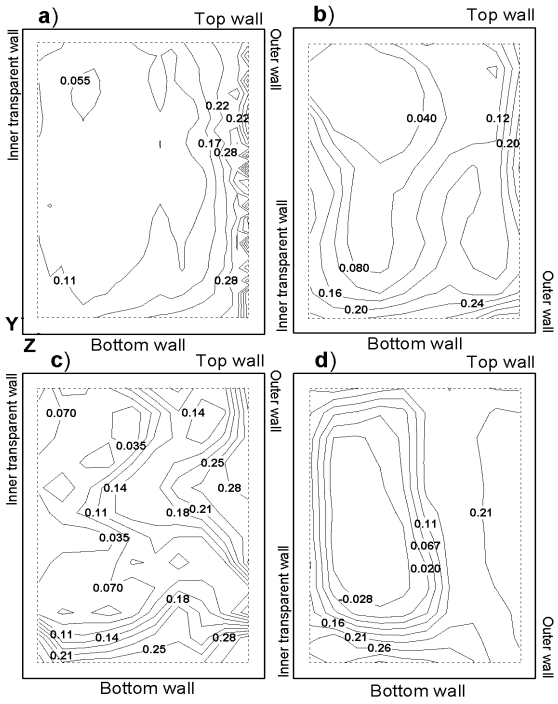

Fig.7 Velocity distributions at the section M_5
(a) ABCD, (b) AD, (c) BD and (d) CD

configuration BD, but was more confined to the inner wall of the diffuser. In the other parts of the measuring section, the flow seemed to reorganise as higher velocities occupied the upper part of the section.

In Fig.6d the presence of screen C in configuration CD eliminated the recirculating zone observed in Fig. 5d, which was probably weakened by the distance from the diffuser inlet and presented higher velocities from the central region of M_4 towards the inner wall.

Velocity Distribution at the Diffuser Outlet

Velocity plot contours presented in Figs 7a–7d permitted the effect of different screen combinations to be determined at the outlet of the diffuser (section M_5). Configuration ABCD presented a velocity distribution with a depleted core region and high-velocity wall layers at the inner wall. Different authors have observed a similar behaviour in diffusers with high-velocity wall layers about the periphery of the diffuser section. Ward–Smith *et al*. [6] described it as wall-jet flow. This wall-jet flow existed for high blockage within the diffuser. In Fig. 7a, the central region of the measuring section had a velocity 60% slower than the one obtained near the inner wall. Configuration AD presented lower velocities near the outer wall and also a relatively depleted central region (Fig. 7b). The flow distribution at the diffuser outlet in configuration CD (Fig.7d) presented a dramatic situation where a large recirculating zone took place near the inner wall. The most uniform velocity distribution obtained, in the present study, was for the configuration BD (Fig.7c) where screen D eliminated the confined recirculating zone observed previously in Fig. 6c.

Static Pressure Distribution

The static pressure loss coefficient profiles for the different configurations can be seen in Fig. 3. Sahin and Ward–Smith [9] reported that perforated plates of low porosity cause high pressure loss and the loss increases as the perforated plates are moved further upstream within the diffuser. As can be seen in Fig. 3, the largest pressure loss occurred in configuration ABCD within the diffuser, even though there was a slight pressure recovery in the region $X/L_1 = 0.6–1.0$, corresponding to the space between screens C and D. In configuration AD, as the flow remained attached the pressure loss coefficient increased within the diffuser. The pressure losses were the lowest in configurations BD and CD. The present results have shown that static pressure measuring at the wall does not give information on the recirculating zones existing between screens in the core region. This fact can be observed in configuration BD where a recovery is observed between locations C and D as the flow was attached to the outer wall, while a recirculating zone existed in the centre region (Fig. 6c). The present pressure results are in good agreement with those obtained by Sahin and Ward–Smith [9] on the use of two perforated plates for flow control within wide-angle diffusers.

Conclusion

Velocity distributions and pressure profiles measured along an asymmetric 30° wide-angle diffuser with an area ratio of 7, were presented for different screen configurations used to achieve flow uniformity at the diffuser outlet. The velocity distributions measured within the diffuser at different locations highlighted the complicated effect of the different blockages seen by the flow within the diffuser. It was found that the location of the first screen had some influence on the velocity profile at the inlet of the diffuser. When the first plate was placed before the separation point at the diffuser inlet, the recirculating zone did not exist downstream, but if the first plate was placed beyond the separation point, the recirculating zone that developed upstream could have some effect on the flow downstream and beyond the perforated plate. A combination of two screens with the same porosity of 45% placed at $X/L_1 = 0.25$ and 0.95 achieved the best velocity uniformity at the outlet for the diffuser under the present study. These results suggest that even an asymmetric diffuser can be used adequately in applications like ESPs where, in most cases, the space and shape allocated to the device depends on other built-up installations. From a fundamental point of view, more theoretical and experimental studies should be devoted to flows within asymmetric diffusers to compare their performance with symmetric systems.

References

[1] Baines, W.D. & Peterson, E.G., An Investigation of Flow Through Screens, *Trans. AMSE*, **50**, 1951, 467–480.

[2] Gibbings, J.C., The Pyramidal Gauze Diffuser, *Ing. Arch. Bd.*, **42**, 1973, 225–233.

[3] Hancock, P.E., Plane Multiple Screens in Non-Uniform Flow With Particular Application to Wind Tunnel Settling Chamber Screens, *Eur. J. Mech. B/Fluids*,**17**, 1998, 357–369.

[4] Sahin, B. & Ward–Smith, A.J., The Use of Perforated Plates to Control the Flow Emerging from a Wide-Angle Diffuser, with Application to Electrostatic Precipitator Design, *J. Heat & Fluid Flow*, **8**, 1987, 124–131.

[5] Sahin, B., Ward–Smith. A.J. & Lane, D., The Pressure Drop and Flow Characteristics of Wide-Angle Screened Diffusers of Large Area Ratio, *J. Wind Eng*., **58**, 1995, 33–50.

[6] Ward–Smith, A.J., Lane, D.L., Reynolds, A.J., Sahin, B. & Shawe D.J., Flow Regimes in Wide-Angle Screened Diffusers, *Int. J. Mech. Sci*., **33**, 1991, 41–54.

[7] Miller, D.S. *Internal Flow Systems*, BHRA, UK, 1990.

[8] Ward–Smith, A.J., *Internal Fluid Flow: The Fluid Dynamics of Flow in Pipes and Ducts*, Clarendon Press, Oxford, 1981.

[9] Sahin, B. & Ward–Smith, A.J., The Pressure Distribution in and Flow Characteristics of Wide-Angle Diffusers Using Perforated Plates for Flow Control with Application to Electrostatic Precipitators, *Int. J. Mech. Sci*., **35**, 1993, 117–127.